Numerical Simulation of the Effect of Variation in Subgrade CBR Values on Rigid Pavement

Suprapto Siswosukarto[1], Muslikh[1], and Taufiq Adi Wijoyo[1*]

[1]*Departement of Civil and Environmental Engineering, Universitas Gadjah Mada, Indonesia*
* Corresponding author: taufiq.adi.w@mail.ugm.ac.id

Abstract: This study presents the results of research on the stress behavior of rigid pavement concrete slabs by varying CBR subgrade values. It aims to know the effect of changing the rigid pavement strss. Data used in this study are geometric data and material properties of the pavement structure. The load vehicle considered is National Road class standard. Rigid pavement is very sensitive with un-uniformity of underlaying supposrt. In this research, the effect of un-uniform support of subgrade was modeled numerically using Abaqus software. The friction coefficient of each layer was also considered in the model. Model simulation of existing rigid pavement calculated 13 variations of CBR values. Result shown that there is a stress increment by 26.27% in the longitudinal direction of the rigid pavement between models with uniform variations of CBR and models with non-uniform variations of CBR. This result show the sensitivity of rigid pavement to un-uniformity of subgrade.

Keywords: *Pavement; CBR; Subgrade; Stress*

1.   Introduction

Rigid pavement is the most suitable type of pavement to be applied to roads with high traffic loads and low soil carrying capacity, because rigid pavements have a much higher stiffness/elastic modulus than flexible pavements, so that the ability to spread the load becomes more even (uniform). Rigid pavement structures consist of cement concrete slabs, with or without a subbase layer placed on the subgrade [1]. Because the subgrade is the lowest supporting layer, the integrity of the pavement structure depends on the stability or carrying capacity of the subgrade [13].

The carrying capacity of the soil is generally influenced by several things, one of which is the level of compaction. Compaction is an attempt to reduce the distance between soil particles, so that voids in the soil filled with air become reduced without reducing the water content. By increasing the density between soil particles, this can increase the carrying capacity and shear strength of the soil [18]. The value of soil density depends on the thickness of the compacted soil layer, the amount of energy of the compactor, and the water content in the soil, the maximum density value can be obtained when the soil moisture content reaches the optimum point. In the design of rigid pavements, the bearing capacity or strength of the soil is represented by the modulus of subgrade reaction obtained from the plate load test or through an approach with an empirical equation that represents the relationship between the modulus of soil reaction and the California bearing ratio value (CBR) [16].

CBR value in granular soils is directly or linearly proportional to the soil density value [17]. Meanwhile, a rigid pavement structure does not require a strong supporting layer as in a flexible pavement structure, but it is far more important to have uniform support [5]. In the design of rigid pavements, the subgrade conditions are assumed to be uniform. There are no rigid pavement analysis guidelines that consider non-uniform subgrade conditions [22]. Meanwhile, during construction, the thickness and water content of the soil were often not well controlled. Testing of soil density which is only carried out at certain points cannot fully represent the condition of the entire area of compacted soil. Thus, the possibility of obtaining a uniform density in the subgrade layer is difficult to realize. The difference in the density of the soil layer can change the stress distribution behavior [6]. Subgrade subject to excessive stress may experience permanent deformation causing damage to the pavement layer. Damage that occurs on rigid pavements can reduce the level of safety and driving comfort, so that it will endanger road users [9].

Based on the description above, in this study modeling the behavior of rigid pavement structures by performing numerical simulations using the 3-dimensional finite element method with computer program tools, namely the Abaqus CAE 6.14 application and analyzing how concrete slabs respond to variations in CBR values on the subgrade. This study also aims to determine the behavior of the stress response on rigid pavements to variations in the CBR value of the subgrade.

2. Method

The rigid pavement data reviewed was obtained from the Central Java PUPR Bina Marga Service. As for the collection of secondary data used in this study in the form of geometric data and material properties of the rigid pavement structure of the roads being reviewed. Apart from that, axle configuration and vehicle load data are also used, as well as other additional data from various literatures. The load used in the simulation of the rigid pavement structure finite element model is MST-10 with a trailer truck load of 1.2-2.2 according to the regulations of the Highways Service Pavement Manual. The tools used in this study were laptops/computers with the Abaqus application with supporting hardware and software.

The modeling parameters used by researchers include:

1. The geometric parameter with the size of the rigid pavement plate is 4 m (transverse) and 5 m (longitudinal) for one plane of the plate and the joints between the rigid pavement plates are tie bars for longitudinal connections and dowels for transverse connections,

2. Material parameters with material values are obtained from the Central Java PUPR Bina Marga Service, material standards from the applicable specifications,

3. Subgrade parameters with uniform subgrade CBR variations (1A Uniform CBR 6%, 1B CBR Uniform 18.23%, 1C CBR Uniform 33.91%),

4. Subgrade parameters with variations in subgrade CBR non-uniform across the road (2A combined CBR 6% and CBR 18.23%, 2B combined CBR 6% and CBR 33.91%, and 2C combined CBR 18.23% and CBR 33.91%),

5. Subgrade parameters with variations in subgrade CBR non-uniform in the longitudinal direction of the road (3A combination of CBR 6% and CBR 18.23%, 3B combination of CBR 6% and CBR 33.91%, and 3C combination of CBR 18.23% and CBR 33.91%),

6. Subgrade parameters with variations in subgrade CBR non-uniform edges (4A combination of CBR 6% and CBR 18.23%, 4B combination of CBR 6% and CBR 33.91%, and 4C combination of CBR 18.23% and CBR 33.91%) and,

7. Parameters of subgrade soil with variations the condition of subgrade CBR values is not uniform randomly with a combination of CBR 6%, CBR 18.23% and CBR 33.91% (Vaviation 5A).

3.   Result and Discussion

3.1. Rigid Pavement Modelling

This study uses a 3D solid model with the Abaqus application. Modeling begins with identifying the parameters to be used in the analysis using Abaqus. The first stage is the Part module, where a Part is made for each layer of rigid pavement with predetermined dimensions. Then, material properties are determined for each Part, including the material definition of the material, material properties in the section, and material calibration [23]. After that, several Parts are combined with Assembly into a unified model, where each Part is independent from one another. Furthermore, in the Step module, users can choose the type of analysis to be used, with this study using material parameters from soil CBR values [4]. In the Interaction module, the user defines the type of interaction between surfaces that meet or have friction [7]. In this research, Tangential Behavior (friction and elastic slip) and Normal Behavior (hard contact, soft contact, damping contact, and separation) are used. In this modeling, the Penalty method is used for limiting contact in the normal direction, where the magnitude of the frictional force is limited to the elastic slip condition when the surface is supposed to stick. In addition, this study included the friction coefficient values for each layer with different values depending on the use of plastic sheets on the surface of the lean concrete and the original pavement layers.
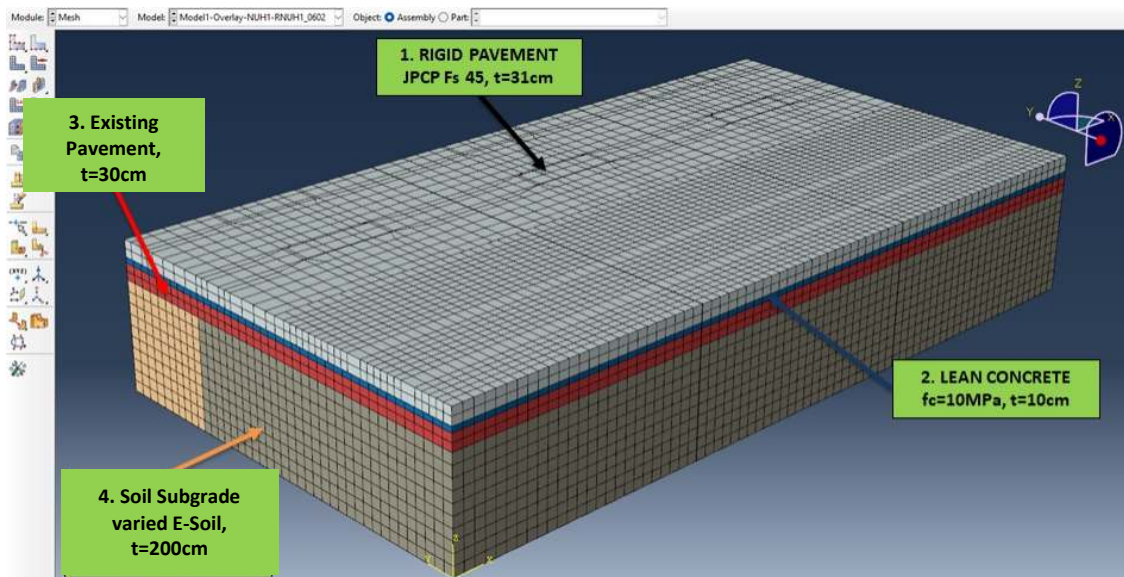

Fig. 1. Rigid Pavement Assembly Model Viewed on Abaqus Software

In the Loads module, trucks weighing 10 tons are used because of their location on the National road class. Boundary conditions used include pins and rollers, in which the entire system can deform vertically except for the subsurface of the subgrade. Boundary joints are applied to the subsurface of the subgrade so as to prevent the subsurface from moving in horizontal and vertical directions. The purpose of the roll boundary conditions is to lock the pavement model so that it does not experience displacement in the x and y directions, even though displacement still occurs, the value will not be too large [15]. The two concrete slabs are also prevented from deforming in the horizontal direction except in the plane of symmetry. Finally, in the Mesh stage, the model structure is divided into elements with a size of 200 mm.

3.2. Response Rigid Pavement Structure Due to Variation in CBR Value

This study uses a truck load with an MST of 10 tons according to Regulation Permen PUPR No. 15/PRT/M/2018. The model created will be analyzed at three loading positions, namely edge, interior, and corner.

3.2.1. Edge Loading Position

Analysis using Abaqus CAE at the edge loading position shows that the variation of Edge Non-uniform (4B) (CBR 6% and CBR 33.91%) produces a maximum stress of 1.50 MPa (tensile) and 1.52 MPa (compression) as seen in Table 1. The values it is still below the limit value f_r and $V_{allowable}$. The deformations at these variations are 0.0689 mm (U1), 0.0487 mm (U2), and 0.976 mm (U3), as shown in Table 2. In addition, the graphs in Fig. 2, Fig. 3 and Fig. 4 show a comparison of the stress between the various loading in the edge loading position.

Table 1. Stresses Due to Edge Loading Positions with Various Variations in CBR Values from Analysis Results on Rigid Pavements using the Finite Element Method

Variation of CBR Values		S11	S22	S33	S12	S13	S23
1A	tensile	1.21	0.88	0.07	0.21	0.21	0.13
	compressive	1.23	1.04	0.46	0.21	0.21	0.16
1B	tensile	0.86	0.63	0.03	0.16	0.19	0.14
	compressive	0.87	0.76	0.47	0.16	0.19	0.15
1C	tensile	0.72	0.52	0.03	0.14	0.18	0.14
	compressive	0.74	0.65	0.47	0.14	0.18	0.14
2A	tensile	1.25	0.84	0.05	0.19	0.22	0.16
	compressive	1.26	1.01	0.53	0.19	0.21	0.17
2B	tensile	1.35	0.88	0.04	0.21	0.23	0.19
	compressive	1.38	1.08	0.62	0.19	0.23	0.20
2C	tensile	0.96	0.66	0.03	0.17	0.20	0.16
	compressive	0.98	0.82	0.53	0.17	0.20	0.17
3A	tensile	1.04	0.69	0.05	0.19	0.22	0.16
	compressive	1.05	0.85	0.53	0.19	0.21	0.18
3B	tensile	1.00	0.86	0.05	0.19	0.23	0.20
	compressive	1.02	1.03	0.71	0.19	0.23	0.20
3C	tensile	0.84	0.54	0.03	0.15	0.20	0.16
	compressive	0.86	0.69	0.53	0.15	0.20	0.17
4A	tensile	1.32	1.11	0.06	0.23	0.24	0.13
	compressive	1.34	1.29	0.53	0.23	0.24	0.18
4B	tensile	1.50	1.35	0.07	0.28	0.27	0.13
	compressive	1.52	1.56	0.62	0.27	0.27	0.22
4C	tensile	0.97	0.76	0.03	0.19	0.22	0.15
	compressive	0.99	0.91	0.53	0.19	0.21	0.17
5A	tensile	1.00	0.74	0.05	0.18	0.23	0.19
	compressive	1.02	0.92	0.62	0.18	0.23	0.20

(units in MPa)

Table 2. Deformation Due to Edge Loading Position with Various CBR Values from Analysis Results on Rigid Pavement using the Finite Element Method

Variation of CBR Values	U1 (mm)	U2 (mm)	U3 (mm)
Uniform 1A	0.062	0.039	0.910
Uniform 1B	0.036	0.020	0.404
Uniform 1C	0.026	0.014	0.250
Transverse non-Uniform 2A	0.048	0.030	0.655
Transverse non-Uniform 2B	0.044	0.028	0.587
Transverse non-Uniform 2C	0.032	0.019	0.354
Longitudinal non-Uniform 3A	0.048	0.031	0.603
Longitudinal non-Uniform 3B	0.043	0.039	0.497
Longitudinal non-Uniform 3C	0.032	0.020	0.327

Variation of CBR Values	U1 (mm)	U2 (mm)	U3 (mm)
Edge non-Uniform 4A	0.063	0.040	0.907
Edge non-Uniform 4B	0.069	0.048	0.976
Edge non-Uniform 4C	0.039	0.022	0.438
Random non-Uniform 5A	0.038	0.026	0.412

Fig. 2. Graph of Maximum Tensile Stress Value Due to Edge Loading Position with Various CBR Value Variations from Analysis Results on Rigid Pavement using the Finite Element Method

Fig. 3. Graph of Maximum Compressive Stress Value Due to Edge Loading Position with Various CBR Value Variations from Analysis Results on Rigid Pavement using the Finite Element Method
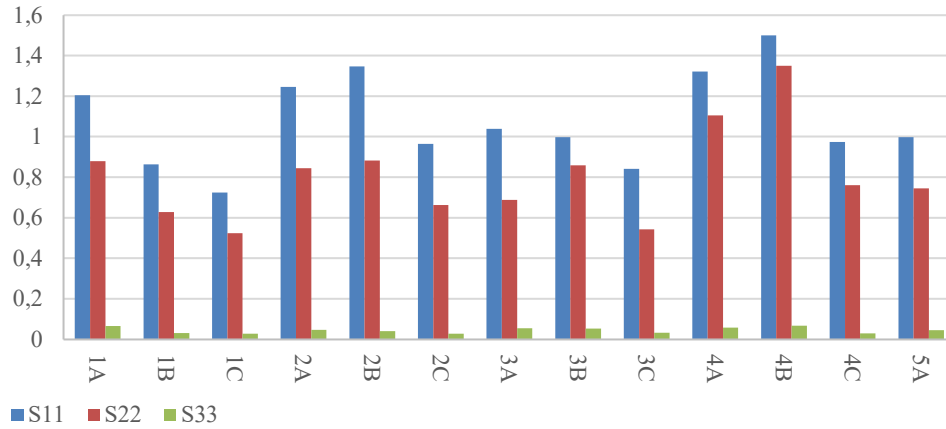

Fig. 4. Graph of Maximum Shear Stress Value Due to Edge Loading Position with Various CBR Value Variations from Analysis Results on Rigid Pavement using the Finite Element Method

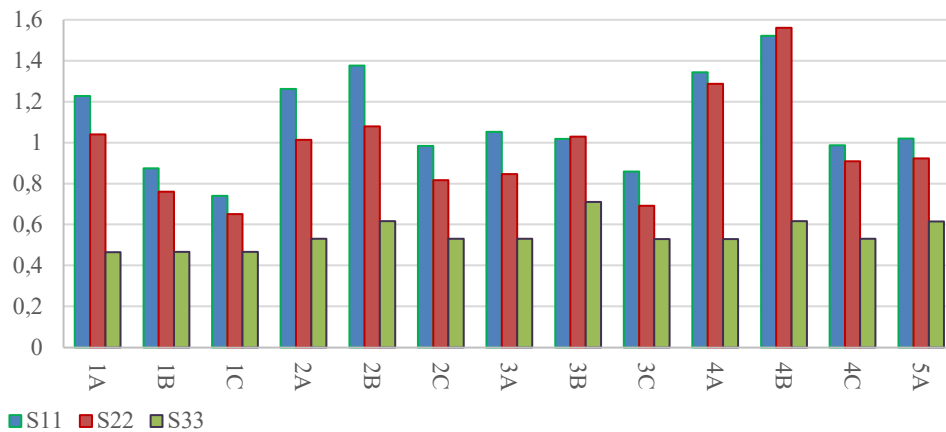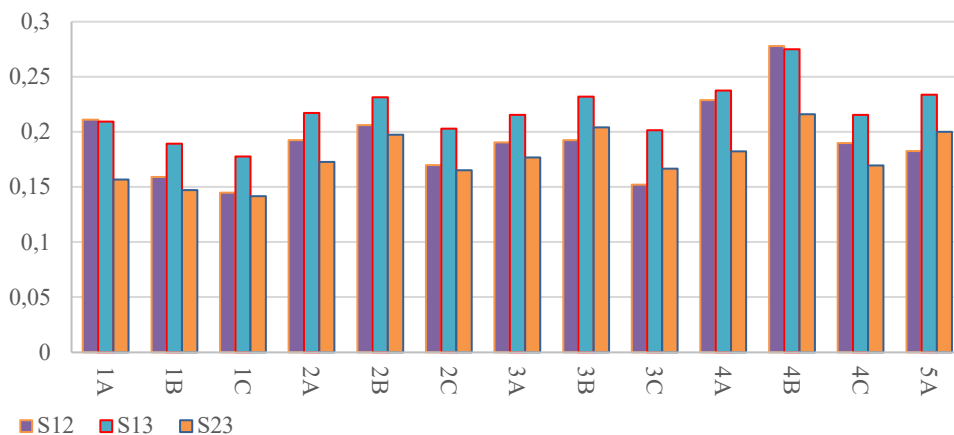Tensile stress and compressive stress of subgrade with uniform CBR values (1A, 1B, 1C) tend to be lower than the cases of variations in CBR values that are not uniform. The transverse non-uniform variations (2A & 2B) and edge non-uniform variations (4A & 4B) produce a relatively higher stress compared to the uniform case (1A). Meanwhile, the transverse non-uniform variation (3C), edge non-uniform variation (4C), and random non-uniform variation (5A) produce higher stresses than the uniform case (1B). Overall, the case of non-uniform variation of edge (4B) with a CBR value of 6% and CBR 33.91% has a higher stress for all the variables analyzed.

3.2.2. Interior Loading Position

At the interior loading position, Table 3. Displays the maximum stress results. In the variation of Edge Non-uniform CBR (4B) (combination of CBR 6% and CBR 33.91%), the tensile stress reaches 0.939 MPa and the compressive stress reaches 1.004 MPa. Compared to the f_r value of 3.894 MPa, these values are still below the f_r value. The maximum shear stress at the same loading position occurs in the variation of Edge Non-uniform CBR (4B) with a tensile stress of 0.190 MPa and a compressive stress of 0.191 MPa. These values are still below the V_{ijin} value of 1.047 MPa. Table 4. Describes the deformation that occurs in the variation of Non-uniform CBR values Edge (4B), with deformation magnitudes of 0.0458 mm in the U1 direction, 0.0312 mm in the U2 direction, and 0.624 mm in the U3 direction.

Table 3. Stress Due to Interior Loading Position with Various CBR Value Variations from the Results of Analysis on Rigid Pavement using the Finite Element Method

Variation of CBR Values		S11	S22	S33	S12	S13	S23
1A	tensile	1.21	0.88	0.07	0.21	0.21	0.13
	compressive	1.23	1.04	0.46	0.21	0.21	0.16
1B	tensile	0.86	0.63	0.03	0.16	0.19	0.14
	compressive	0.87	0.76	0.47	0.16	0.19	0.15
1C	tensile	0.72	0.52	0.03	0.14	0.18	0.14
	compressive	0.74	0.65	0.47	0.14	0.18	0.14
2A	tensile	1.25	0.84	0.05	0.19	0.22	0.16
	compressive	1.26	1.01	0.53	0.19	0.21	0.17
2B	tensile	1.35	0.88	0.04	0.21	0.23	0.19
	compressive	1.38	1.08	0.62	0.19	0.23	0.20
2C	tensile	0.96	0.66	0.03	0.17	0.20	0.16
	compressive	0.98	0.82	0.53	0.17	0.20	0.17
3A	tensile	1.04	0.69	0.05	0.19	0.22	0.16
	compressive	1.05	0.85	0.53	0.19	0.21	0.18
3B	tensile	1.00	0.86	0.05	0.19	0.23	0.20
	compressive	1.02	1.03	0.71	0.19	0.23	0.20
3C	tensile	0.84	0.54	0.03	0.15	0.20	0.16
	compressive	0.86	0.69	0.53	0.15	0.20	0.17
4A	tensile	1.32	1.11	0.06	0.23	0.24	0.13
	compressive	1.34	1.29	0.53	0.23	0.24	0.18
4B	tensile	1.50	1.35	0.07	0.28	0.27	0.13
	compressive	1.52	1.56	0.62	0.27	0.27	0.22
4C	tensile	0.97	0.76	0.03	0.19	0.22	0.15
	compressive	0.99	0.91	0.53	0.19	0.21	0.17
5A	tensile	1.00	0.74	0.05	0.18	0.23	0.19
	compressive	1.02	0.92	0.62	0.18	0.23	0.20

(units in MPa)

Table 4. Deformation Due to Interior Loading Position with Various CBR Value Variations from the Results of Analysis on Rigid Pavement using the Finite Element Method

Variation of CBR Values	U1 (mm)	U2 (mm)	U3 (mm)
Uniform 1A	0.062	0.039	0.910
Uniform 1B	0.036	0.020	0.404
Uniform 1C	0.026	0.014	0.250
Transverse non-Uniform 2A	0.048	0.030	0.655
Transverse non-Uniform 2B	0.044	0.028	0.587
Transverse non-Uniform 2C	0.032	0.019	0.354
Longitudinal non-Uniform 3A	0.048	0.031	0.603
Longitudinal non-Uniform 3B	0.043	0.039	0.497
Longitudinal non-Uniform 3C	0.032	0.020	0.327
Edge non-Uniform 4A	0.063	0.040	0.907
Edge non-Uniform 4B	0.069	0.048	0.976
Edge non-Uniform 4C	0.039	0.022	0.438
Random non-Uniform 5A	0.038	0.026	0.412

Fig. 5. Graph of Maximum Tensile Stress Value Due to Interior Loading Position with Various CBR Value Variations from Analysis Results on Rigid Pavement using the Finite Element Method

Fig. 6. Graph of Maximum Compressive Stress Value Due to Interior Loading Position with Various CBR Value Variations from Analysis Results on Rigid Pavement using the Finite Element Method
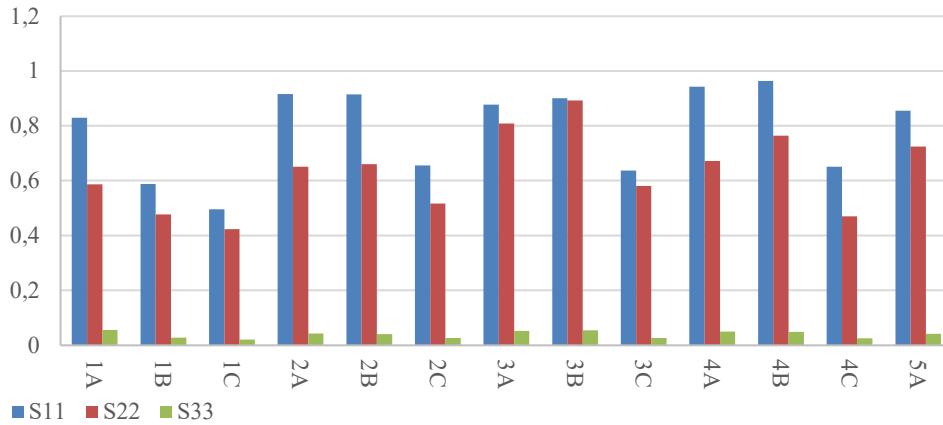
Fig. 7. Graph of Maximum Shear Stress Value Due to Interior Loading Position with Various CBR Value Variations from Analysis Results on Rigid Pavement using the Finite Element Method
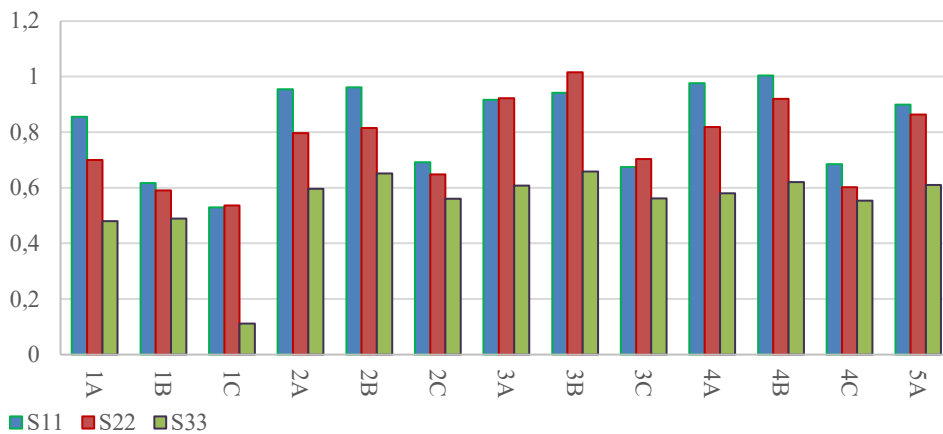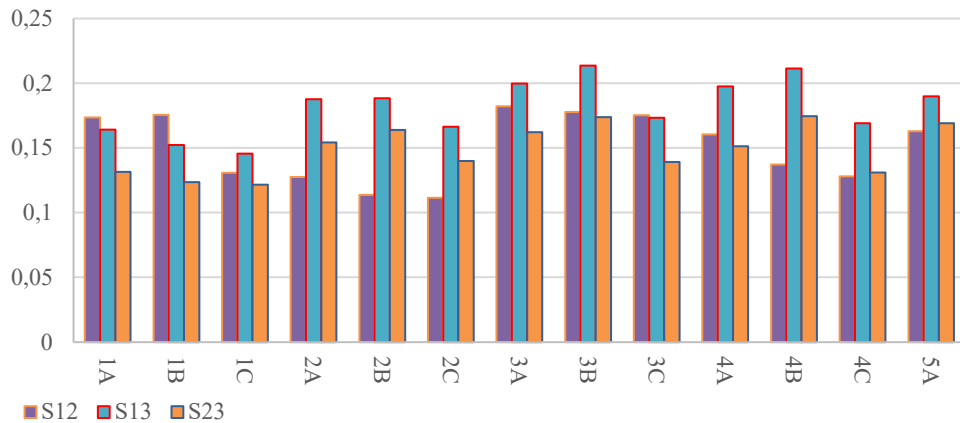
Fig. 5., Fig. 6 and Fig. 7. Shows a graph of the stress comparison between loading variations at the interior loading position. In this analysis, subgrade soils with uniform CBR values (1A, 1B, 1C) have lower tensile and compressive stresses compared to most cases of non-uniform CBR values. The case of transverse non-uniform variation (2A & 2B) and edge non-uniform variation (4A & 4B) produce higher stresses than the uniform case (1A). The transverse non-uniform variation (3C), edge non-uniform variation (4C), and random non-uniform variation (5A) also produce higher stresses compared to the uniform case (1B). However, the longitudinal non-uniform variations (3A, 3B & 3C) produce lower voltages compared to the uniform case (1A & 1B). Overall, the case of non-uniform variation of edge (4B) with a CBR value of 6% and CBR 33.91% has a higher stress value for all the variables analyzed.

3.2.3. Corner Loading Position

Through Table 5. The results of the analysis at the corner loading position show the maximum stress when varying the non-uniform CBR value of Edge (4B) with a combination of 6% CBR and 33.91% CBR. The tensile stress reaches 1.33 MPa and the compressive stress is 1.37 MPa. Nonetheless, these values are still below the f_r value of 3.894 MPa. The maximum shear stress also occurs at edge non-uniform variation (4B) with the same CBR value, namely 0.297 MPa for tensile stress and 0.299 MPa for compressive stress. These values are also below the $V_{allowable}$ value of 1.047 MPa. The deformations that occur in these variations can be seen in Table 6, with magnitudes of 0.0874 mm in the U1 direction, 0.0542 mm in the U2 direction, and 1.067 mm in the U3 direction.

Table 5. Stress Due to Interior Loading Position with Various CBR Value Variations from the Results of Analysis on Rigid Pavement using the Finite Element Method

Variation of CBR Values		S11	S22	S33	S12	S13	S23
1A	tensile	1.05	0.88	0.20	0.21	0.21	0.21
	compressive	1.08	1.04	0.76	0.22	0.20	0.21
1B	tensile	0.78	0.65	0.17	0.16	0.19	0.21
	compressive	0.80	0.78	0.69	0.15	0.16	0.20
1C	tensile	0.66	0.56	0.02	0.14	0.18	0.21
	compressive	0.69	0.67	0.66	0.14	0.14	0.20
2A	tensile	1.25	0.98	0.22	0.27	0.27	0.25
	compressive	1.29	1.18	0.96	0.27	0.23	0.27
2B	tensile	1.27	1.12	0.25	0.31	0.30	0.25

Variation of CBR Values		S11	S22	S33	S12	S13	S23
2C	compressive	1.31	1.32	1.00	0.32	0.26	0.30
	tensile	0.96	0.66	0.03	0.17	0.20	0.16
	compressive	0.98	0.82	0.53	0.17	0.20	0.17
3A	tensile	1.00	0.83	0.17	0.23	0.23	0.27
	compressive	1.03	0.99	0.87	0.23	0.20	0.27
3B	tensile	0.90	0.97	0.21	0.23	0.23	0.29
	compressive	0.93	1.13	0.91	0.23	0.18	0.30
3C	tensile	0.77	0.63	0.16	0.15	0.20	0.24
	compressive	0.80	0.75	0.75	0.15	0.16	0.24
4A	tensile	1.26	1.22	0.27	0.25	0.25	0.22
	compressive	1.29	1.43	0.97	0.26	0.24	0.23
4B	tensile	1.33	1.39	0.31	0.30	0.27	0.21
	compressive	1.37	1.62	1.06	0.30	0.26	0.25
4C	tensile	0.88	0.79	0.20	0.19	0.21	0.23
	compressive	0.91	0.94	0.80	0.19	0.18	0.21
5A	tensile	0.84	0.89	0.19	0.21	0.22	0.27
	compressive	0.87	1.04	0.85	0.21	0.17	0.28

(units in MPa)

Table 6. Deformation Due to Interior Loading Position with Various CBR Value Variations from the Results of Analysis on Rigid Pavement using the Finite Element Method

| Variation of CBR Values	U1 (mm)	U2 (mm)	U3 (mm)
Uniform 1A	0.076	0.044	0.976
Uniform 1B	0.042	0.024	0.443
Uniform 1C	0.030	0.019	0.287
Transverse non-Uniform 2A	0.081	0.049	1.042
Transverse non-Uniform 2B	0.092	0.054	1.202
Transverse non-Uniform 2C	0.032	0.019	0.354
Longitudinal non-Uniform 3A	0.062	0.038	0.691
Longitudinal non-Uniform 3B	0.050	0.033	0.537
Longitudinal non-Uniform 3C	0.037	0.024	0.363
Edge non-Uniform 4A	0.086	0.049	1.062
Edge non-Uniform 4B	0.087	0.542	1.067
Edge non-Uniform 4C	0.046	0.029	0.483
Random non-Uniform 5A	0.046	0.031	0.489
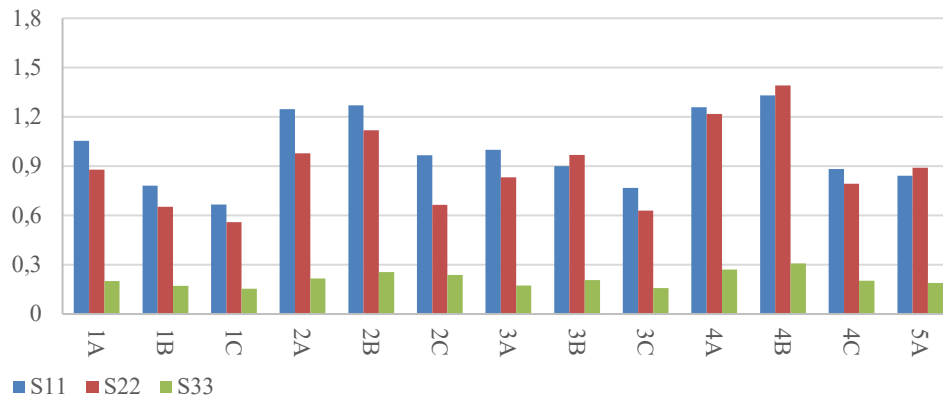
Fig. 8. Graph of Maximum Tensile Stress Value Due to Corner Loading Position with Various CBR Value Variations from Analysis Results on Rigid Pavement using the Finite Element Method
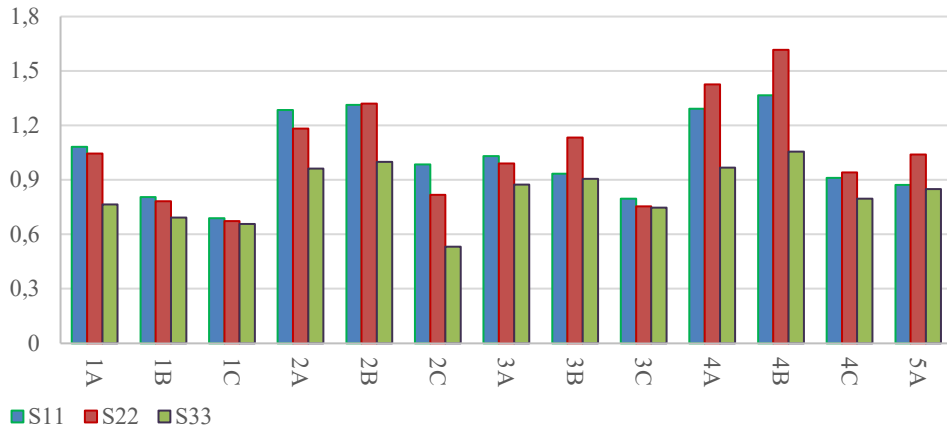
Fig. 9. Graph of Maximum Compressive Stress Value Due to Corner Loading Position with Various CBR Value Variations from the Results of Analysis on Rigid Pavement using the Finite Element Method

Fig. 10. Graph of Maximum Shear Stress Value Due to Corner Loading Position with Various CBR Value Variations from the Results of Analysis on Rigid Pavement using the Finite Element Method
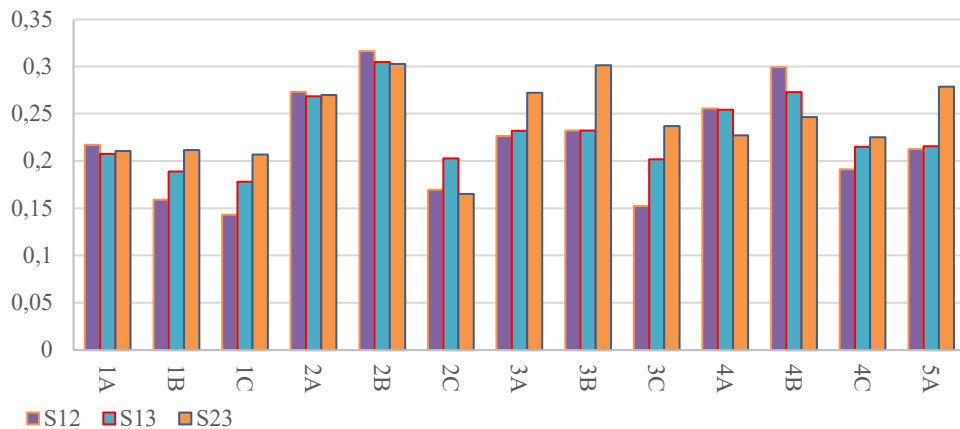
Through Fig. 7., Fig. 8 and Fig. 9., it can be seen a graph that compares the stress values between loading variations at the corner loading positions. It can be seen that the subgrade with uniform CBR values (1A, 1B, 1C) has relatively lower tensile and compressive stresses compared to most cases of non-uniform CBR values. The cases of transverse non-uniform variations (2A & 2B) and edge non-uniform variations (4A & 4B) produce relatively higher stresses than the uniform cases (1A). While the transverse non-uniform variation (3C), edge non-uniform variation (4C), and random non-uniform variation (5A) produce a relatively higher stress than the uniform case (1B). Overall, the case of non-uniform variation of edge 4B with a CBR value of 6% and CBR 33.91% has a higher stress value for all the variables analyzed.

In addition, based on the analysis carried out on the given variables, cases of variations in Edge Non-uniform CBR values (4B) (combination of CBR 6% and CBR 33.91%) have stress values both tensile and compressive which are greater than other cases, both cases uniform and non-uniform CBR values in all loading positions [19] [14]. This indicates that there is an increase in voltage of 26.27% for voltage S11, 58.44% for voltage S22 and 54.65% for voltage S33. The results of this study indicate that there is an influence between the non-uniformity of the CBR value on the stresses that occur in rigid pavement structures (concrete slabs). These results are also in line with previous studies which showed that stiff subgrade with soft edges and subgrade with random soft and stiff locations significantly increased the tensile stress by about 32% compared to suniform soft subgrade conditions [3]. This is confirmed form another research, where the existing traffic loads are loaded on the edges and interior positions on the pavement tend to

have a lower stress than the stresses at the corners [11]. As is well known, for angular loading conditions, the principal tensile stress is at the top of the slab and at the corner of the circular load area. This is because, with the application of these loads a "cantilever" type mechanism occurs for the slab which naturally generates greater stresses at the top of the structure and near the supports.

Table 7. Deformation Due to Interior Loading Position with Various CBR Value Variations from the Results of Analysis on Rigid Pavement using the Finite Element Method

		Stress Variation 1A on Corner Load (MPa)	**Stress Variation 4A on Corner Load (MPa)**	**Stress Increment**
		(a)	(b)	$[(b) - (a)]/(a)$
S11	tensile	1.053	1.330	26.31%
	compressive	1.081	1.365	**26.27%**
S22	tensile	0.877	1.390	**58.44%**
	compressive	1.044	1.615	54.69%
S33	tensile	0.199	0.308	**54.65%**
	compressive	0.764	1.055	38.14%
S12	tensile	0.213	0.297	39.50%
	compressive	0.217	0.299	37.88%
S13	tensile	0.207	0.273	31.64%
	compressive	0.199	0.259	29.75%
S23	tensile	0.208	0.211	1.10%
	compressive	0.210	0.246	17.06%

The non-uniformity of the CBR value can affect the stresses that occur in rigid pavement structures, such as concrete slabs, because CBR is one of the important factors affecting the bearing capacity of the subgrade or soil under the pavement [2]. The non-uniformity of the CBR value can lead to the non-uniformity of the bearing capacity of the soil under the pavement. This means that some sections of the pavement will experience higher loads than others. When a load is applied to a pavement, stresses will occur in it. If there is non-uniformity in the bearing capacity of the subgrade, the stresses that occur in the pavement will also be uneven. Uneven stresses in pavements can cause structural problems such as cracks or deformation [8]. Pavement sections subjected to higher loads will experience greater stresses, increasing the risk of cracking or structural damage. Meanwhile, sections of pavement that are subjected to lower loads may not be subjected to sufficient stress to support the traffic passing through them.

3.3. Fatigue Analysis

Fatigue is a condition of reduced strength in a material caused by cyclically applied tensile loads which are usually below the yield strength of the material. The concept of Portland Cement Association (PCA) fatigue analysis is to avoid pavement failure (or initiation of the first crack) by fatigue of concrete due to repetition of critical stresses. The 1984 PCA fatigue analysis, calculated the estimated value of N_f as follows [2]

$$f_r = 0.62\,\lambda\,\sqrt{f'c} \tag{1}$$

$$f_r = 0.62\,(1)\sqrt{(39.45)} = 3.894 \text{MPa}$$

$$Stress\ Ratio\ (SR) = \frac{\sigma}{M_R} \tag{2}$$

$$\text{if } SR \geq 0.55 \text{ then, } \log N_f = 11.737 - 12.077\,SR \tag{3}$$

if $0.45 < SR < 0.55$ then, $N_f = \frac{4.2577}{SR - 0.4325}$ (4)

if $SR < 0.45$ then, $N_f = \infty$ (5)

From the results of the fatigue analysis that has been carried out, the results are in the form of the maximum number of repetitions of the load that can be accepted by rigid pavements. From Table 8, it can be seen that the rigid pavement at the edge loading position has the highest fatigue effect on the condition of variations in the Non-uniform CBR value of Edge 4B with the largest stress ratio (SR) value of 40.1% resulting in the smallest load repetition value of 2.23×10^{10} according to the method StreetPave where the value is more influential than the condition of the CBR Uniform (1A) value variation, namely 4.32×10^{17} according to the StreetPave method and Uniform (1C), namely 2.58×10^{54} according to the StreetPave method. The load received by the pavement will be more concentrated compared to the center of the pavement [12]. Edge loading tends to result in higher loads along the edges and lower loads in the center of the pavement. When there are variations in CBR values that are not uniform at the edges, areas with low CBR will support higher loads, while areas with high CBR will support lower loads. This causes a significant stress difference along the pavement edge. In addition, the loads that are also applied to rigid pavements, the stresses that occur will concentrate in certain areas that experience higher loads [10]. Under edge loading, stresses will concentrate along the pavement edges and spread into the pavement structure. When there are variations in the CBR value that are not uniform at the edges, areas with low CBR will experience greater stress, while areas with high CBR will experience lower stress. High stresses in areas of low CBR can cause pavement damage and fatigue.

Table 8. Deformation Due to Interior Loading Position with Various CBR Value Variations from the Results of Analysis on Rigid Pavement using the Finite Element Method

Variation of CBR Values		σ_{max} (MPa)	σ_{max} / f_r	Repetition (N_f)	
				Method PCA	Method StreetPave
1A	tensile	1.21	0.31	unlimited	2.5×10^{18}
	compressive	1.23	0.32	unlimited	4.3×10^{17}
1B	tensile	0.86	0.22	unlimited	3.4×10^{38}
	compressive	0.87	0.22	unlimited	3.0×10^{37}
1C	tensile	0.72	0.19	unlimited	9.2×10^{56}
	compressive	0.74	0.19	unlimited	2.6×10^{54}
2A	tensile	1.25	0.32	unlimited	1.3×10^{17}
	compressive	1.26	0.32	unlimited	4.0×10^{16}
2B	tensile	1.25	0.32	unlimited	1.3×10^{17}
	compressive	1.38	0.35	unlimited	4.7×10^{13}
2C	tensile	0.96	0.25	unlimited	1.4×10^{30}
	compressive	0.98	0.25	unlimited	7.4×10^{28}
3A	tensile	1.04	0.27	unlimited	3.7×10^{25}
	compressive	1.05	0.27	unlimited	7.4×10^{24}
3B	tensile	1.00	0.26	unlimited	1.1×10^{28}
	compressive	1.03	0.26	unlimited	1.2×10^{26}
3C	tensile	0.84	0.22	unlimited	7.2×10^{40}
	compressive	0.86	0.22	unlimited	1.1×10^{39}
4A	tensile	1.32	0.34	unlimited	9.3×10^{14}
	compressive	1.34	0.35	unlimited	2.7×10^{14}
4B	tensile	1.50	0.39	unlimited	2.0×10^{11}
	compressive	1.56	0.40	unlimited	2.2×10^{10}
4C	tensile	0.97	0.25	unlimited	3.5×10^{29}

Variation of CBR Values		σ_{max} (MPa)	σ_{max} / f_r	Repetition (N_f)	
				Method PCA	Method StreetPave
	compressive	0.99	0.25	unlimited	4.9×10^{28}
5A	tensile	1.00	0.26	unlimited	9.9×10^{27}
	compressive	1.02	0.26	unlimited	4.3×10^{26}

From Table 9., it can be seen that at the interior loading position, the rigid pavement has the highest fatigue effect on the condition of variations in the Non-uniform CBR Edge (4B). The largest value of the stress ratio (SR) is 25.8%, resulting in the smallest load repetitions of 3.88×10^{27} according to the StreetPave method, where this value is smaller / more influential than the condition of the CBR value variation of Uniform variation (1A) with load repetitions of 2.48×10^{39} and Uniform variation (1C) with load repetitions of 1.24×10^{111} according to the StreetPave method.

Table 9. Fatigue Analysis of Interior Loading Positions with Various Variations in CBR Values from Analysis Results on Rigid Pavement

Variation of CBR Values		σ_{max} (MPa)	σ_{max} / f_r	Repetition (N_f)	
				Method PCA	Method StreetPave
1A	tensile	0.829	0.213	unlimited	1.51×10^{42}
	compressive	0.855	0.220	unlimited	2.48×10^{39}
1B	tensile	0.587	0.151	unlimited	7.22×10^{90}
	compressive	0.616	0.158	unlimited	3.98×10^{81}
1C	tensile	0.496	0.127	unlimited	3.19×10^{132}
	compressive	0.536	0.138	unlimited	1.24×10^{111}
2A	tensile	0.916	0.235	unlimited	6.97×10^{33}
	compressive	0.954	0.245	unlimited	8.04×10^{30}
2B	tensile	0.916	0.235	unlimited	6.97×10^{33}
	compressive	0.961	0.247	unlimited	2.56×10^{30}
2C	tensile	0.655	0.168	unlimited	2.21×10^{71}
	compressive	0.691	0.178	unlimited	1.59×10^{63}
3A	tensile	0.877	0.225	unlimited	1.78×10^{37}
	compressive	0.921	0.237	unlimited	2.44×10^{33}
3B	tensile	0.900	0.231	unlimited	1.57×10^{35}
	compressive	1.015	0.261	unlimited	8.49×10^{26}
3C	tensile	0.636	0.163	unlimited	1.23×10^{76}
	compressive	0.703	0.181	unlimited	7.39×10^{60}
4A	tensile	0.942	0.242	unlimited	6.23×10^{31}
	compressive	0.976	0.251	unlimited	2.39×10^{29}
4B	tensile	0.964	0.248	unlimited	1.60×10^{30}
	compressive	1.004	0.258	unlimited	3.88×10^{27}
4C	tensile	0.650	0.167	unlimited	2.79×10^{72}
	compressive	0.685	0.176	unlimited	3.16×10^{64}
5A	tensile	0.855	0.220	unlimited	2.66×10^{39}
	compressive	0.899	0.231	unlimited	1.88×10^{35}

Furthermore, in Table 10, it can be seen that if the rigid pavement in the angular loading position has the highest fatigue effect on conditions of variations in the Non-uniform CBR Edge (4B) with the largest stress ratio (SR) value of 41.5% resulting in the smallest load repetition value of 3.93×10^9 according to the StreetPave method where the value is smaller / more influential than the condition of the variation in the CBR value of Uniform 1A, namely 2.58×10^{23} according to

the StreetPave method and Uniform variation (1C), namely 7.52×10^{63} according to the StreetPave method.

Table 10. Fatigue Analysis of Corner Loading Positions with Various Variations in CBR Values from Analysis Results on Rigid Pavement

Variation of CBR Values		σ_{max} (MPa)	σ_{max} / f_r	Repetition (N_f)	
				Method PCA	Method StreetPave
1A	tensile	1.053	0.270	unlimited	6.56×10^{24}
	compressive	1.081	0.278	unlimited	2.58×10^{23}
1B	tensile	0.780	0.200	unlimited	2.22×10^{48}
	compressive	0.805	0.207	unlimited	1.33×10^{45}
1C	tensile	0.664	0.171	unlimited	1.12×10^{69}
	compressive	0.688	0.177	unlimited	7.52×10^{63}
2A	tensile	1.246	0.320	unlimited	1.19×10^{17}
	compressive	1.285	0.330	unlimited	8.79×10^{15}
2B	tensile	1.246	0.320	unlimited	1.19×10^{17}
	compressive	1.320	0.339	unlimited	1.05×10^{15}
2C	tensile	0.965	0.248	unlimited	1.36×10^{30}
	compressive	0.984	0.253	unlimited	7.42×10^{28}
3A	tensile	0.998	0.256	unlimited	9.10×10^{27}
	compressive	1.031	0.265	unlimited	1.02×10^{26}
3B	tensile	0.968	0.249	unlimited	8.21×10^{29}
	compressive	1.132	0.291	unlimited	1.35×10^{21}
3C	tensile	0.767	0.197	unlimited	1.34×10^{50}
	compressive	0.795	0.204	unlimited	1.95×10^{46}
4A	tensile	1.258	0.323	unlimited	5.18×10^{16}
	compressive	1.425	0.366	unlimited	4.68×10^{12}
4B	tensile	1.390	0.357	unlimited	2.46×10^{13}
	compressive	1.615	0.415	unlimited	3.93×10^{9}
4C	tensile	0.882	0.226	unlimited	6.48×10^{36}
	compressive	0.941	0.242	unlimited	7.67×10^{31}
5A	tensile	0.889	0.228	unlimited	1.33×10^{36}
	compressive	1.040	0.267	unlimited	3.25×10^{25}

From the results of the analysis above, it can be seen that for conditions of variation in CBR values and loading positions that have the greatest influence in this study are conditions of variation in CBR values Non-uniform Edge 4B with corner loading positions with the largest stress ratio (SR) value of 41.5% and the value that can be borne by a rigid pavement is 3.93×10^{9} according to the StreetPave method, while the PCA method produces unlimited values. The condition of variation in CBR values is not uniform [21]. Edges are the biggest influence on the conditions of variation in CBR values and loading positions because the loads that occur on rigid pavements can cause structural fatigue. When there is a non-uniform variation of the CBR value at the edges, the area with low CBR will experience greater stress repeatedly from the load, which has the potential to cause fatigue to occur more quickly.

4. Conclusion

Equations for mathematical formulation should be center and numbered with the number on the right-hand side.

The purpose of this study was to investigate the response of rigid pavement slab structures due to various factors, namely vehicle loads and subgrade CBR variations. These factors are combined

in the analysis of the finite element method to produce that the maximum stress on the rigid pavement is found in variation 4B at an angle loading of 1.615 MPa in the transverse direction. The voltage that occurs is still below fr. The deformation value in the stress case is 1.067 mm in the pavement thickness direction. The results show that there is an increase in the stress value of 26.27% in the longitudinal direction of the rigid pavement between models with uniform CBR value variations and models with non-uniform CBR value variations. These results indicate the sensitivity of the stress on the pavement concrete slab due to the non-uniformity of the subgrade CBR values.

Based on the results of the research and analysis carried out, there are suggestions and recommendations recommended by the authors, namely the implementation process must strictly measure the CBR value so that there is no difference in the CBR value. If a difference in the CBR value is found, it must be repaired immediately before it causes damage that affects the service condition of the pavement. Furthermore, to obtain analysis results that are close to conditions that occur in the field, the effect of temperature should be carried out in further research so that the results of the analysis are close to the original conditions in the field. Research is also proposed to be carried out on a new rigid pavement that is built on native soil so as to produce an ideal rigid pavement layer.

References

[1] Amakye, S. Y. O., Abbey, S. J., & Booth, C. A. (2022). Road pavement defect investigation using treated and untreated expansive road subgrade materials with varying plasticity index. *Transportation Engineering*, 9, 100123. https://doi.org/10.1016/j.treng.2022.100123

[2] Baadiga, R., Balunaini, U. (2023). Evaluation of pavement design input parameters of biaxial and triaxial geogrid stabilized flexible pavements overlying soft subgrades. *Cleaner Materials*, 9, 100192. https://doi.org/10.1016/j.clema.2023.100192

[3] Brand, A. S., Roesler, J., Chavan, H. L., & Evangelista, F. J. (2013). Effects of a Non-Uniform Subgrade Support on the Response of Concrete Pavement, *Report Departement*, Iowa: Iowa University.

[4] Chou, J.S. (2009). Web-based CBR system applied to early cost budgeting for pavement maintenance project. *Expert Systems with Applications*, 36(2), 2947–2960. https://doi.org/10.1016/j.eswa.2008.01.025

[5] Delatte, N. (2008). *Concrete Pavement Design, Construction, and Performance*. New York : Taylor & Francis.

[6] Hardiyatmo, H. C. (2015). *Road Pavement Design and Soil Investigation*. Yogyakarta: Gadjah Mada University Press. (in Indonesia)

[7] Hu, Y., Zhu, H., Li, J. (2023). Effect of solution road Romix Soilfix on deformation performance of granular base material: A laboratory and field investigation. *Construction and Building Materials*, 393, 131894.https://doi.org/10.1016/j.conbuildmat.2023.131894

[8] Klekovkina, M., Gorshkov, V., & Lialinov, A. (2017). Development of Methods for Evaluating the Impact of Stress-Strain State Uniformity of Composite Pavements on Road Safety. *Transportation Research Procedia, 20*, 301-304. https://doi.org/10.1016/j.trpro.2017.01.027

[9] Luo, W., Wang, K. C. P., Li, L., Li, Q. J., & Moravec, M. (2014). Surface Drainage Evaluation for Rigid Pavements Using an Inertial Measurement Unit and 1-mm Three-Dimensional Texture Data. *Transportation Research Record*, 2457(1), 121–128. https://doi.org/10.3141/2457-13

[10] Lv,S., Tan, L., Peng, X., Hu, L., Liu, H., Yuan, J., Wang, S. (2021). Fatigue resistance design of rubberized asphalt mixture pavement under three-dimensional stress state. *Construction and Building Materials, 307*, 125138. https://doi.org/10.1016/j.conbuildmat.2021.125138

[11] Mahfuda, A., Siswosukarto, S., Suhendro, B., (2023). The Influence of Temperature Variations on Rigid Pavement Concrete Slabs. *Journal of the Civil Engineering Forum, May 2023*, 9(2):139-150. https://doi.org/10.22146/jcef.5744

[12] Mascio, P.D., Moretti, L., Capannolo, A. (2019). Concrete block pavements in urban and local roads: Analysis of stress-strain condition and proposal for a catalogue. *Journal of Traffic and Transportation Engineering (English Edition), 6(6)*, 557-566. https://doi.org/10.1016/j.jtte.2018.06.003

[13] Pasetto, M. Giacomello, G. Baliello, A., Pasquini, E. (2023). An Italian road pavement design method for bus lanes: proposal and application to case studies. *Transportation Research Procedia, 69*, 847-854. https://doi.org/10.1016/j.trpro.2023.02.244

[14] Pradhan, S.K & Biswal, G. (2021). Utilization of reclaimed asphalt pavement (RAP) as granular sub-base material in road construction. *Materials today: proceedings, 60(1)*, 288-293 https://doi.org/10.1016/j.matpr.2021.12.564

[15] Prawesti, P., Suhendro, B., Hapsoro, S. (2019). Evaluation of rigid pavement on apron of terminal 3 Soekarno-Hatta International Airport using finite element method. *MATEC Web of Conferences 270, 03005, 2019*. https://doi.org/10.1051/matecconf/201927003005

[16] Praveen, G. V., Kurre, P., & Chandrabai, T. (2020). Improvement of California Bearing Ratio (CBR) value of Steel Fiber reinforced Cement modified Marginal Soil for pavement subgrade admixed with Fly Ash. *Materials today: proceedings.* https://doi.org/10.1016/j.matpr.2020.08.814

[17] Saffar, A. K. K. Al, Behaya, S. A. M., Jassim, H. S. H., & Ajam, H. K. K. (2021). Empirical Equation Correlate California Bearing Ratio (CBR) with Dry Density for Granular Soil. *Academia.Edu*, 10(07), 300–303.

[18] Saniga, A.M., Rajish, A., Shankar, S., Vishnu, R. (2023). Optimal pavement maintenance and management strategies for flood affected low volume rural roads. *Materials today: Proceedings*. https://doi.org/10.1016/j.matpr.2023.05.187

[19] Shen, Z.,Liu, B., Zhou, G. (2022). Stressing state analysis of concrete airport pavement by modeling experimental strain data. *Case Studies in Construction Materials, 17*, e01635. https://doi.org/10.1016/j.cscm.2022.e01635

[20] Titus-Glover, L., Mallela, J., Darter, M., Voigt, G., Waalkes, S. (2005). Enhanced Portland Cement Concrete Fatigue Model for StreetPave. *Transportation Research Record: Journal of the Transportation Research Board, 1919*, 29-37. 10.1177/0361198105191900104.

[21] Toribio, J., Tino, R., González, B., Franco, M., Carlos,J. (2022). Structural integrity of hot bituminous mixtures for road pavements: mechanical and environmental factors governing fatigue & fracture. *Procedia Structural Integrity, 37*, 985-988. https://doi.org/10.1016/j.prostr.2022.02.034

[22] Vishwakarma, R. J., & Ingle, R. K. (2020). *Effect of non-uniform soil subgrade on critical stresses in concrete pavement-Lecture Notes in Civil Engineering*. Singapore: Springer.

[23] Zokaei-Ashtiani, A., Carrasco, C., & Nazarian, S. (2014). Finite element modeling of slab–foundation interaction on rigid pavement applications. *Computers and Geotechnics, 62,* 118–127. https://doi.org/10.1016/j.compgeo.2014.07.003